Eur. Phys. J. B **5**, 169–178 (1998)

THE EUROPEAN PHYSICAL JOURNAL B

Soft modes and phonon interactions in $Sn_2P_2S_6$ studied by neutron scattering

S.W.H. Eijt[1a,b], R. Currat[2], J.E. Lorenzo[3], P. Saint-Grégoire[4], B. Hennion[5], and Yu.M. Vysochanskii[6]

[1] Research Institute for Materials, University of Nijmegen, Toernooiveld, 6525 ED Nijmegen, The Netherlands
[2] Institut Laue-Langevin, BP 156X, 38042 Grenoble Cedex, France
[3] CNRS Laboratoire de Cristallographie, BP 166, 38042 Grenoble Cedex, France
[4] Université Toulon-Var, BP 132, 83957 La Garde Cedex, and CEMES[c], BP 4347, 31055 Toulouse Cedex, France
[5] Laboratoire Léon Brillouin, CEA/Saclay, 91191 Gif-Sur-Yvette, France
[6] Institute for Physics and Chemistry of Solid State, Uzhgorod State University, 294000 Uzhgorod, Ukraine

Received: 11 May 1998 / Revised and Accepted: 15 June 1998

Abstract. The low frequency lattice dynamics and its relationship to the second order paraelectric-to-ferroelectric transition in $Sn_2P_2S_6$ is studied. The dispersion branches of the acoustic and lowest lying optical phonons in the a^*-c^* plane have been obtained in the ferroelectric phase, for x-polarized phonons. Close to the phase transition a considerable softening is found for the lowest optical mode (P_x), comparable to the behaviour observed in previous Raman investigations. As found previously in $Sn_2P_2Se_6$, a strong coupling between the TO(P_x) and TA(u_{xz}) phonons is observed, although, apparently, not strong enough to lead to an incommensurate phase. The soft TO(P_x) mode at the zone center is observed. The temperature dependence of its frequency and damping shows that the transition is not entirely displacive. At low temperatures an unusual apparent negative LO-TO splitting is observed which is shown to arise from the coupling of the x-polarized soft mode to the nearby z-polarized optical phonon. For comparison, the soft TO(P_x) dispersion in the a^*-b^* plane is measured in both the paraelectric and ferroelectric phases. Consistent frequency changes and LO-TO splitting are observed, revealing a significant interaction between the TA(u_{yx}) and LA(u_{xx}) acoustics branches and the TO and LO soft optic branches, respectively. In contrast, the nearby y-polarized optic branch shows almost no temperature dependence. Finally, the influence of piezoelectric effects on the limiting acoustic slopes in the ferroelectric phase is discussed.

PACS. 64.70.Kb Solid-solid transitions – 61.12.-q Neutron scattering – 63.20.Dj Phonon states and bands, normal modes, and phonon dispersion – 63.20.Kr Phonon-electron and phonon-phonon interactions – 61.44.Fw Incommensurate crystals

1 Introduction

Ferroelectric phase transitions have received considerable attention with respect to their structural and dynamical aspects, as for example in $BaTiO_3$ [1] and Thiourea [2]. In particular the existence of soft modes and/or order-disorder mechanisms has been the object of numerous optical and neutron spectroscopic studies. In certain systems, of which the so-called type II incommensurate proper ferroelectrics are examples, an incommensurate (IC) phase appears between the high temperature (symmetric) phase and the ferroelectric phase. BCCD [3], $NaNO_2$ [4], Thiourea [2] and $Sn_2P_2Se_6$ [5] are examples of this class of systems. Type II means that the thermodynamic potential contains no Lifshitz invariant. Hence, in such systems the incommensurate phase is viewed as arising [6] from the interaction of the ferroelectric soft optic mode with an acoustic mode [3] or with another optic phonon [7], creating an instability at non-zero wavevector just outside the Brillouin zone center.

Indeed, in a previous paper [5] it was shown that the incommensurate phase formation in $Sn_2P_2Se_6$ is a result of a strong coupling between the TO (P_x polarisation) soft optic phonon and the TA(u_{xz} strain) acoustic phonon, propagating along the c^* direction.

The $Sn_2P_2(S_{1-x}Se_x)_6$ family of uniaxial ferroelectrics is an excellent model system to study the appearance of an intermediate IC phase. Mixed crystals can be grown for all values of $x\,(0 < x < 1)$. $Sn_2P_2Se_6$ ($x = 1$) shows an intermediate incommensurate phase at ambient pressure, in contrast to $Sn_2P_2S_6$ ($x = 0$) (Fig. 1). The latter undergoes a direct second order phase transition at $T_0 = 337$ K between a paraelectric phase ($P2_1/n$) and a ferroelectric

[a] *Present address:* CNRS/MPI Grenoble High Magnetic Field Laboratory, BP 166, 38042 Grenoble Cedex 9, France.
[b] e-mail: eijt@labs.polycnrs-gre.fr
[c] UPR CNRS 8011.

phase (Pn, $n = \left(\frac{1}{2}\ 0\ \frac{1}{2}\right)$ for both). An important question is therefore, why an incommensurate phase occurs in $Sn_2P_2Se_6$, and not in $Sn_2P_2S_6$, with a rare Lifshitz point [8] in the x-T phase diagram ($x_L = 0.28$; $T_L = 288$ K), at which the period of modulation is expected to become infinite [8].

It is well-known from lattice dynamical studies [9] that the structural changes in ferroelectric phase transitions bear a close relationship to the vibrational displacements associated with the high temperature phase soft mode. The changes in structure between the paraelectric and ferroelectric phases have been well studied for $Sn_2P_2S_6$ [10,11] and $Sn_2P_2Se_6$ [12,13] using X-ray crystallographic techniques. Throughout the paper we use the pseudo-orthorhombic setting of Rizak *et al.* [14]: $a = 9.318$ Å, $b = 7.463$ Å, $c = 6.518$ Å, $\alpha = \gamma = 90°$, $\beta = 91.15°$ ($Sn_2P_2S_6$, 358 K). Upon transition to the ferroelectric phase, the main changes consist of pairwise displacements of the Sn atoms, approximately along the a-axis, relative to the rigid P_2S_6 groups, destroying the inversion symmetry and the twofold axis. The B_u symmetry of the displacements results in the appearance of a dielectric polarisation in the a-c plane at an angle of 15° with the a-axis.

The soft mode behaviour in $Sn_2P_2S_6$ has been studied by Raman [15], infrared [16] and dielectric spectroscopy [17]. The acoustic properties were investigated by ultrasound measurements [18,19] and Brillouin scattering [20]. All experimental results indicate that the transition is mainly displacive. In $Sn_2P_2S_6$ the existence of a soft mode in the ferroelectric phase has clearly been demonstrated by Raman and infrared spectroscopy. The soft mode appears not to soften completely (about 0.35 THz at T_0). Infrared measurements in the paraelectric phase of $Sn_2P_2S_6$ indicate an overdamped B_u soft mode at about 0.4 THz, slowly varying with temperature. However, the analysis is rather problematic due to a strong low frequency wing partly obscuring the soft phonon response. The origin of the wing is still unclear and might reflect a coupling of the soft mode to a lower frequency excitation or an order-disorder component in the neighbourhood of T_0.

Further indications that the soft mode might contain an order-disorder component come from Brillouin scattering, where the LA(u_{zz}) response shows evidence of a coupling to a low frequency excitation or a central peak close to T_0. Also, specific heat measurements [21] reveal a large transition entropy at the second order phase transition temperatures T_i (crystals with $x \geq x_L$) and T_0 (crystals with $x \leq x_L$), typical of an order-disorder transition.

Inelastic neutron scattering is a very suitable technique to study the soft mode properties in both paraelectric and ferroelectric phases, not suffering from problems and limitations met with the optical techniques: Raman spectroscopy on the one hand is not sensitive to the B_u soft mode of the centrosymmetric phase, while the infrared spectroscopic data [16] on the other hand, do not allow to extract unambiguous soft mode parameters due to the contribution of the low frequency wing mentioned above.

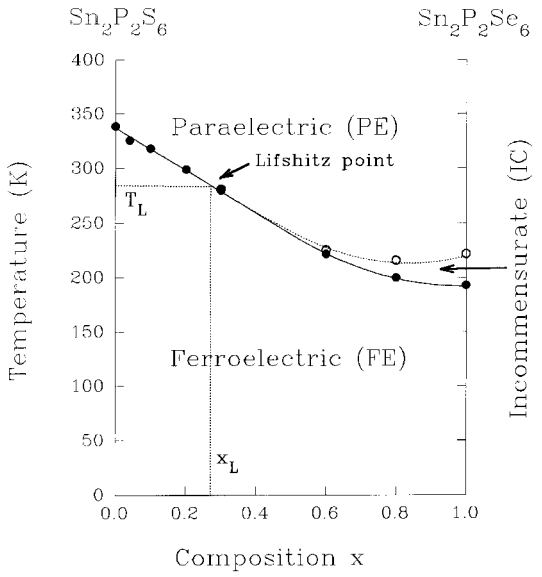

Fig. 1. Composition-temperature phase diagram of $Sn_2P_2(S_{1-x}Se_x)_6$ [8].

Another unsettled problem is the microscopic character of the forces leading to the incommensurate transition. Previous lattice dynamical calculations [14] were based on zone center frequencies only, which is clearly insufficient. Although the calculations could simulate a strong anisotropy of the a^*-c^* low frequency branches, with a soft direction along the incommensurate wave vector direction, this occured only simultaneous to the erroneous prediction of an instability along the b-axis. Beside dipole-dipole interactions, changes in the short range repulsive interactions upon replacing the S-atoms by the (larger) Se-atoms are believed to be essential in order to explain the incommensurate phase formation in $Sn_2P_2Se_6$, and not in $Sn_2P_2S_6$ [14].

In this study of $Sn_2P_2S_6$ it is shown that a clear soft mode behaviour is observed in connection with the ferroelectric phase, and that as in $Sn_2P_2Se_6$, the coupling of the soft optic x-polarized phonon with acoustic and other optic phonons is strong.

An intriguing aspect of the Raman results by Gommonai *et al.* [22], is the fact that the soft mode in the ferroelectric phase of $Sn_2P_2S_6$ has a complicated temperature and directional dependence in the a^*-c^*, as well as in the a^*-b^* planes. This was tentatively attributed to angular dispersion associated with the LO-TO splitting together with strong anisotropic interactions of the soft TO (P_x) mode with the nearby optic modes of P_y and P_z polarization.

All these open questions motivated the present neutron scattering study. Here, the dynamics of $Sn_2P_2S_6$ in both the paraelectric and ferroelectric phase is investigated. The soft mode parameters are extracted as a function of temperature. The dispersion properties in the a^*-c^* plane (ferroelectric phase) and a^*-b^* plane (ferroelectric

and paraelectric phases) are presented. Finally, the piezoelectric contributions to the acoustic velocities for this strongly piezoelectric crystal (in the ferroelectric phase) are discussed.

2 Experimental

Two single crystals of $Sn_2P_2S_6$ (respectively 1 and 2 cm^3) were used. The crystals were grown by the Bridgmann technique. The sulfur-based crystals are normally optically transparent with a slight pink coloration, in contrast to the selenium-based crystals which show metallic reflection. The crystalline quality of the specimens investigated was found to be adequate by neutron diffraction standards, with no detectable mosaic structure or twinning.

Experiments were carried out on several thermal and cold-source three-axis neutron spectrometers at ILL-Grenoble (France), (IN3, IN12 and IN14) and LLB-Saclay (France), (1T1). Several closed-cycle He-refrigerators and cryofurnaces were used during the course of the measurements, with typical temperature homogeneity and stability of a fraction of a Kelvin.

Inelastic constant-Q measurements were performed in both the energy gain and energy loss modes. The instrumental energy resolution was adjusted to match the experimental requirements, by varying the incident and scattered neutron energies (from 5 to 14 meV), as well as the neutron beam collimations.

3 Lattice dynamics of $Sn_2P_2S_6$

The low frequency phonon dispersion branches of $Sn_2P_2S_6$ in the a^*-c^* plane were studied on IN12 at four temperatures (200 K, 250 K, 320 K and 330 K) in the ferroelectric phase, mainly in the Brillouin zones (5 0 -1) and (3 0 1). The phonon wavevector was selected along c^* as well as a^* in order to probe both the transverse and longitudinal behaviour of phonons polarised along a.

These geometries have been selected for two reasons. First, since the same were used for $Sn_2P_2Se_6$, in order to provide a direct comparison of the dynamics of the two crystals, useful in the understanding of the Lifshitz point occurrence. The modulation wavevector of the latter compound lies in the a^*-c^* plane, close to c^*. Secondly, the macroscopic polarisation in the ferroelectric phase in both compounds is approximately along a^*. Therefore the soft TO mode in both the ferroelectric and paraelectric phases is expected to be observable for $\mathbf{q}//c^*$. In addition, the low frequency lattice dynamics has been investigated in the a^*-b^* plane in order to identify the low frequency optic mode dispersions. Raman studies [22–25] showed the presence of three closely spaced optic modes, assigned as the x-polarized soft mode, and a y- and a z-polarized optic mode.

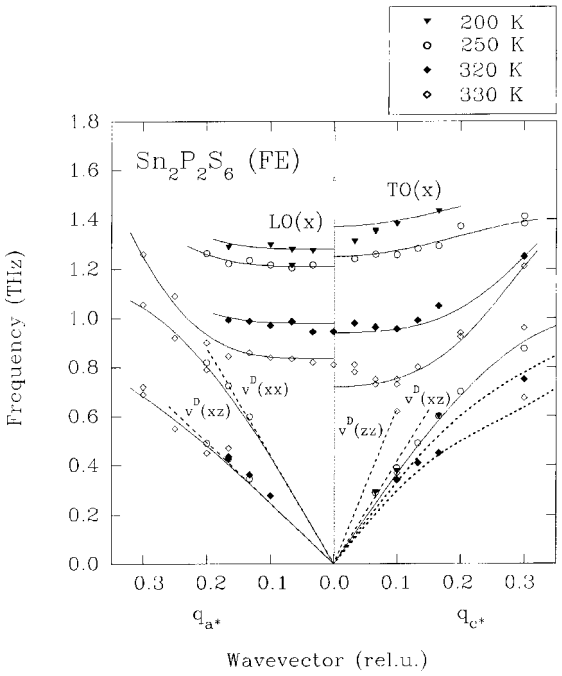

Fig. 2. Low frequency phonon dispersion of $Sn_2P_2S_6$ in the ferroelectric phase as function of temperature (errorbars typically ± 0.04 THz) obtained from DHO-fits. The soft TO phonon and the transverse acoustic TA(xz) branch (dashed lines) show a clear repulsion upon approaching T_0. Solid lines and short dashed lines are guides to the eyes.

3.1 Dispersion curves in the a*-c* plane

Figure 2 shows the temperature evolution of the low frequency dispersion curves of $Sn_2P_2S_6$ in the ferroelectric phase, for 4 temperatures. The symmetry of the various modes in the a^*-c^* plane was described in [5]. The frequencies were obtained by careful fitting of the phonon spectra to damped harmonic oscillator lineshapes, including Gaussian responses for elastic incoherent scattering and Bragg contributions at low q values.

Clearly it can be observed that the TO(x) and LO(x) branches decrease in frequency upon heating the crystal in the ferroelectric phase towards T_0, demonstrating a clear soft mode behaviour. For non-zero wavevector the TO branch decreases much faster than the LO branch. At zero wavevector ($q = 0$) it appears that the branches meet continuously, presumably related to a resolution artifact. Due to the finite q-resolution both the LO and TO responses contribute close to $q = 0$, resulting in a complex lineshape, and an intermediate frequency is therefore obtained in the spectral analysis. This effect was accounted for by extrapolating the branches towards $q = 0$, as shown by the solid lines in Figure 2.

A remarkable feature is the apparently negative LO-TO splitting at low temperatures ($\nu(TO) > \nu(LO)$ at 200 K), which becomes positive only in the neighbourhood of the phase transition. To the authors knowledge, no other experimental observation of an inverted polar

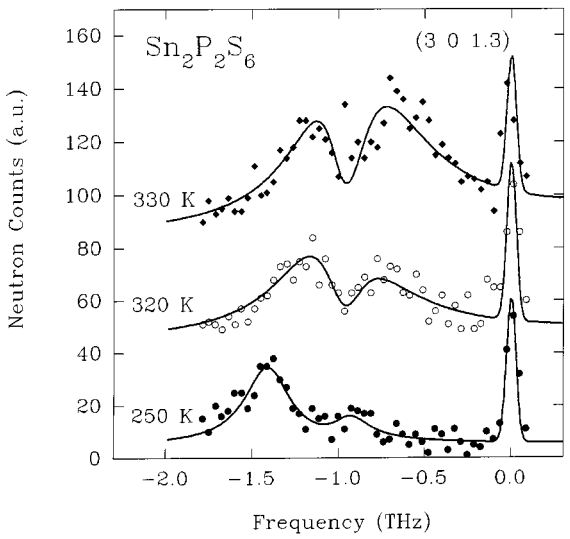

Fig. 3. Temperature evolution of the $k_f^3 \cot(\phi_f)$-corrected spectra at (3 0 1.3) showing the interaction between the TO and TA phonons. Solid lines present CDHO-line shape simulations.

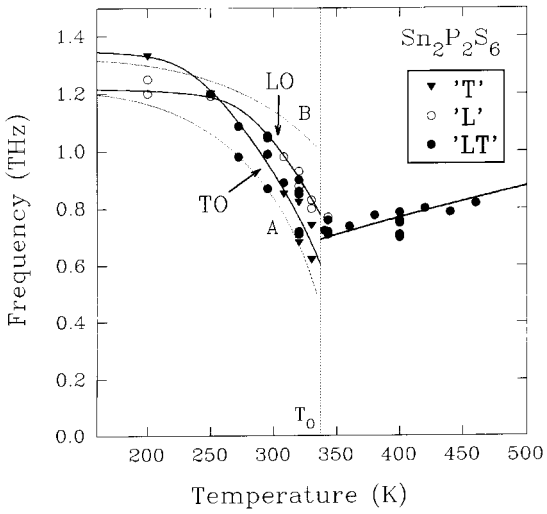

Fig. 4. Temperature dependence of the soft mode frequency. The solid lines (fits according to the model described by Eq. (3)) are drawn according to ω_{TO}^2=0.0135($T_0 - T$) + 0.39 THz^2, ω_{LO}^2=0.0135($T_0 - T$)+0.65 THz^2 and ω_{para}^2=0.0018($T_0 - T$) + 0.49 THz^2, respectively, including the interaction to the z-polarised LO and TO phonon (at 1.36 and 1.22 THz, respectively) in the ferroelectric phase. The A and B modes (dashed lines) observed in backscattering Raman experiments (Gommonai *et al.* [22,23]) have been included for comparison (see text).

vibration is present in the literature (see *e.g.* [26–28] for discussion and examples of LO-TO splittings). A similar effect is however present in the related compound $Sn_2P_2Se_6$ [5]. The soft optic dispersion in $Sn_2P_2S_6$ and $Sn_2P_2Se_6$ does not obey the usual temperature behaviour [22]:

$$\omega^2(q, \alpha, T) = A|T - T_c| + Bq^2 + C\cos^2\alpha \qquad (1)$$

in which α is the angle between the phonon wavevector $\mathbf{q}$ and the spontaneous polarisation $\mathbf{P}_s$ in the xz or xy plane, and C is the LO-TO splitting, which in this approximation is constant as a function of temperature. In the Raman experiments by Gommonai *et al.* [22] substantial deviations of the soft mode frequency $\omega^2(q, \alpha, T)$ from equation (1) have been found as well, with respect to both angular and temperature dependences.

There are a few possible explanations for the apparent negative LO-TO splitting. One is the presence of another excitation at low frequencies, which contributes to the dielectric properties in the soft mode frequency range. If the resulting real part of the dielectric constant ϵ' is negative, an inverted LO-TO order may result. However, at low temperatures such an excitation was absent in both infrared and Raman experiments. In Section 3.2 it will be shown that the negative LO-TO splitting may more probably result from a coupling of the x-polarized soft mode and the nearby z-polarized optic phonon, as suggested by Gommonai *et al.* [22]. In both cases under consideration, the Lyddane-Sachs-Teller-relationship remains valid when all relevant modes are included.

Besides the overall softening of the TO branch, its dispersion shows clear changes with temperature. At 250 K the branch is quite flat, whereas at 320 K a strong dispersion with wavevector q_{c^*} is observed. At the same time, the TA(xz) branch is clearly repelled towards lower frequencies, indicative of a TO-TA phonon interaction.

This is supported by clearly observable spectral features typical of mode interaction, for example in the temperature dependence of the (3 0 ±1.3) spectra (Fig. 3). At low temperatures, the TO soft mode is strong, whereas the TA mode is barely visible. As the temperature is raised the TO phonon moves down in frequency, transfering part of its intensity to a lower frequency maximum at approximately the TA(xz) frequency and showing repulsion effects. It is clear that the TO and TA phonons interact, quite similar to the interaction observed in the paraelectric phase of $Sn_2P_2Se_6$.

Therefore the TO-TA spectra were analysed using the coupled damped harmonic oscillator (CDHO) response, using the procedure described in a previous paper on $Sn_2P_2Se_6$ [5]. Figure 3 shows that the CDHO model accounts satisfactorily for the observed spectral features.

3.2 Temperature behaviour of the soft phonon

In Figures 4 and 5 the temperature behaviour of the LO(x) and TO(x) frequency and damping in the paraelectric and ferroelectric phases is shown. In the paraelectric phase the soft mode, studied in the zone center of the (3 0 1) Brillouin zone, exhibits a slow frequency decrease upon approaching the phase transition. In the ferroelectric phase the soft mode was studied in the (3 0 ±1) and (5 0 ±1) zones. The observed frequencies and damping are categorized as transverse "T" ($q_{c^*} = 0.1\,c^*$), longitudinal "L"

($q_{a^*} = 0.1\,a^*$) and mixed longitudinal-transverse "LT" (zone center measurement). The soft mode in the paraelectric phase stabilizes at a frequency intermediate between the extrapolated LO (0.78 ± 0.05 THz) and TO (0.60 ± 0.05 THz) frequencies of the ferroelectric phase, showing that the paraelectric response (at $q = 0$) is a superposition of the LO- and TO-components. No attempts were made to determine the LO-TO splitting existing in the paraelectric phase, which should be of same size as in the ferroelectric phase close to the transition. The observed temperature behaviour is nevertheless illustrative of the soft mode frequency changes in the paraelectric phase.

In the ferroelectric phase the TO-phonon ($q_{c^*} = 0.1c^*$) changes close to T_0 as $\omega^2 = a'(T_0 - T) + d'$, in which $a' = 0.0135 \pm 0.002$ THz^2/K and $d' = 0.39 \pm 0.05$ THz^2. The frequency in the paraelectric phase is analysed by a similar temperature behaviour $\omega^2 = a(T - T_0) + d$, where $a = 0.0018 \pm 0.0005$ THz^2/K (similar to $Sn_2P_2Se_6$) and $d = 0.49 \pm 0.04$ THz^2. The relative ferroelectric-to-paraelectric soft mode frequency changes in $Sn_2P_2S_6$ are much larger
$(R = \dfrac{d\omega^2}{dT}(T_0^-)/\dfrac{d\omega^2}{dT}(T_0^+) = -7.5 \pm 2.5)$ than expected on the basis of a ϕ^4 potential ($R = -2$).

In this respect it is interesting to note that $Sn_2P_2S_6$ is close to a tricritical point, where the fourth order term in the thermodynamic potential vanishes [29]. Consequently, the (virtual) paraelectric-to-ferroelectric transition changes from second order ($Sn_2P_2S_6$) to first order ($Sn_2P_2Se_6$). Since the thermodynamic potential and the soft mode potential are related, it can be expected that terms higher than fourth order contribute significantly to the soft mode anharmonic potential. The deviation from $R = -2$ might alternatively be related to the presence of order-disorder effects. This has been shown by molecular dynamics simulations of anharmonic systems [30]. Indications for order-disorder effects in both $Sn_2P_2S_6$ and $Sn_2P_2Se_6$ are indeed found in a number of experimental investigations: specific heat indicates a large transition entropy [21] and Brillouin spectra showed features of a central peak [20]. Note that the soft mode LO-TO splitting found here is relatively small (about 0.16 THz near T_0), which in part might be related to the negative splitting observed at low temperatures. The dielectric contribution of the B_u optic modes, deduced by IR methods [16], was found to be more than one order of magnitude lower than the dielectric constant near the phase transition.

A comparison of the present results with infrared [16] and Raman [15,22] data indicates a lower soft mode frequency near T_0 (about 0.4 THz) in the optical work. However, the analysis of the Raman and infrared (IR) spectra is obscured by the presence of a low frequency wing, especially strong just below T_0 and (in IR) in a wide temperature range above the transition. The temperature variation of the soft mode frequency in both phases is similar to that deduced from the neutron experiment, although the Raman analysis results in a 15% faster ω^2 change in the ferroelectric phase.

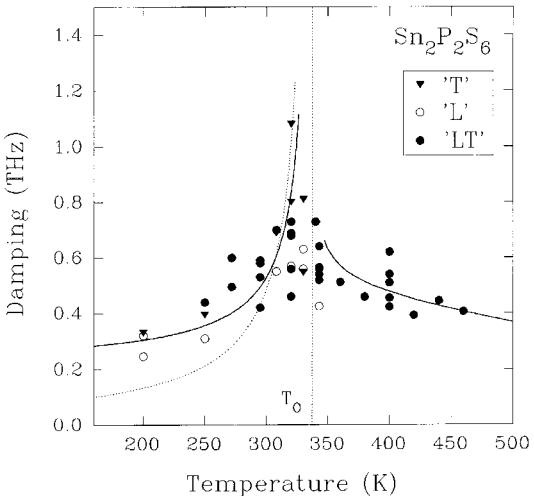

Fig. 5. Temperature dependence of the soft mode damping. Full lines are the theoretical damping curves including the resolution (0.25 THz) of the neutron experiment. The dashed line in the ferroelectric phase shows the damping values deduced from the Raman data in [15].

The damping shows the usual increase upon approaching the ferroelectric phase transition from both sides (Fig. 5). In the ferroelectric phase the temperature evolution of the damping is compared to predictions based on third order anharmonic decay of the optic phonon into acoustic phonons [31], allowing a comparison with a similar analysis of the Raman spectra by Vysochanskii *et al.* [15]:

$$\Gamma = a\frac{T}{\sqrt{T_0 - T}} + b\frac{T}{T_0 - T} + c. \qquad (2)$$

Using similar parameters as in [15] (here we find: $a \approx 0.006$ THz$/\sqrt{K}$, $b \approx 0.015$ THz and $c \approx 0.049$ THz) the prediction from equation (2) convoluted with the resolution width w_R of the neutron experiment is shown as solid lines in Figure 5 ($w_R \approx 0.25$ THz). The dashed line in the ferroelectric phase denotes the temperature behaviour observed in the Raman experiment ($w_R \approx 0.04$ THz), which is in reasonable agreement with the damping values found here. Clearly, the LO mode has a lower damping close to T_0.

As in the case of $Sn_2P_2Se_6$, the damping constant in the paraelectric phase shows a weaker temperature dependence, consistent with the slower rate of change of the paraelectric soft mode frequency.

Below 250 K, both LO- and TO-frequencies saturate near 1.4 THz, and an apparent negative LO-TO splitting is observed. As stated earlier, this can be explained by a coupling of the x-polarized soft mode to the nearby z-polarized polar phonon, as shown by the model presented below.

The model is further motivated by the outcome of Raman and polariton scattering experiments [22,32], where a strong anisotropy in the behaviour of the low frequency optic branches is observed, whose origin was tentatively

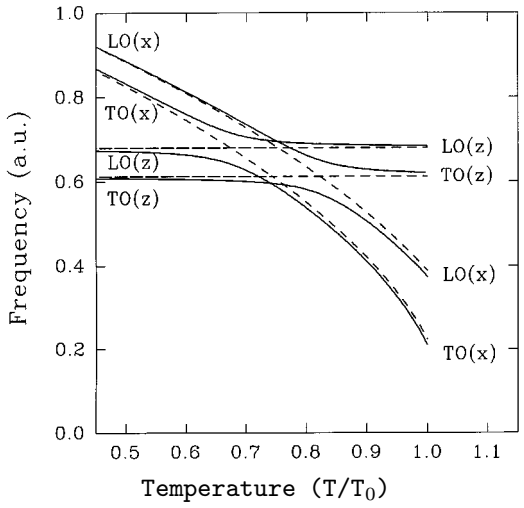

Fig. 6. Model of the x-polarised and z-polarised phonon-interaction resulting in an apparently negative LO-TO(x) splitting at low temperature ($T/T_0 \leq 0.7$).

attributed to such a coupling mechanism. It was shown that both y-polarized (A''-symmetry) and z-polarized (A'-symmetry) polar optic mode frequencies lie close to the soft mode.

Our model assumes a positive LO-TO splitting for both x- and z-polarized phonons (Fig. 6); a possible coupling to the y-polarized optic mode is ruled out by symmetry. The thermodynamic potential Φ allows two types of interaction terms, an analytical (in (q_x, q_z)) isotropic term, dP_xP_z, and a non-analytical interaction term $f\frac{q_xq_z}{q^2}P_xP_z$, which is only strong for wave vector directions intermediate between x and z. This results in the following dynamical matrix:

$$\mathbf{D} = \begin{pmatrix} \omega_x^2(q,\alpha,T) & d + f\cos\alpha\sin\alpha \\ d + f\cos\alpha\sin\alpha & \omega_z^2 \end{pmatrix}$$

$$= \begin{pmatrix} \omega_x^2(q,\alpha,T) & d' \\ d' & \omega_z^2 \end{pmatrix} \quad (3)$$

in which $\omega_x^2(q,\alpha,T)$ is described by equation (1). The interaction $d' = d + f\cos\alpha\sin\alpha$ results in a repulsion of the two phonons. In the neutron experiments the wave vector was selected $q//c^*$, not exactly perpendicular to the polarisation P_x ($\alpha \cong 76°$), showing that, in principle, both coupling terms may contribute.

In Figure 6 the qualitative temperature dependence of the LO and TO parts of the soft mode have been depicted according to this model, assuming constant A, C and d', coupled to a temperature independent z-polarized optic phonon. At low temperatures the z-polarized phonon is assumed to be at slightly lower frequencies than the x-polarized phonon. As the temperature is raised, the LO(z) first interacts with the TO(x) phonon and at somewhat higher temperatures the TO(z) interacts with the LO(x) phonon. Consequently, the apparently repelled LO(x) (lowest curve in Fig. 6 for $\frac{T}{T_0} \leq 0.7$) is lower in frequency than the TO(x) at low temperatures, thus explaining the observed negative LO-TO splitting. Close to T_0, in contrast, the TO (P_x) shows an normal softening.

Fits of the soft mode frequencies according to the model described by the 2×2 dynamical matrix of equation (3) are shown by the solid lines in Figure 4. A constant interaction strength $d' = 0.2$ THz^2 is assumed together with temperature independent bare mode frequencies 1.36 THz (LO(z)) and 1.22 THz (TO(z)), respectively.

The LO(x) temperature dependence is nearly the same as obtained in Raman studies [22] (not shown). In contrast, close to the phase transition, the TO(x) mode follows the A-mode observed in the Raman study of Gommonai *et al.* [22], who assigned it as the TO(x) soft mode. At lower temperatures a disagreement between the neutron and Raman results occurs, where the neutron data show that the soft mode follows more closely the B-mode observed in the Raman study (which was assigned as the TO(z)-mode).

Two reasons could explain the discrepancy. Firstly, since the Raman results are obtained at much lower q-values than the neutron results, an additional dispersion in the low q-range could be present. On the other hand, the neutron data are more likely to show the correct soft mode behaviour since a direct relationship between Raman tensor elements and mode assignment does not exists. The neutron data indicate a change of the soft mode polarisation from the x-direction to a direction in the plane including a z-component. The latter would explain moreover the anomalous behaviour of the B-mode at low temperatures (below 100 K) [22], where it shows a predominant frequency increase, up to 1.36 THz. In contrast, the A-mode is temperature independent in the same range.

Additional neutron studies, in particular on z-polarized vibrations, are necessary to verify this conjecture and to clarify the anisotropic behaviour of the Raman scattering spectra in detail.

In the discussion one should not underestimate the influence on the resulting lineshapes of the interaction of the soft mode, both with the z-polarized optic phonon and with the TA(xz) acoustic phonon. An interesting example is the investigation of the soft mode behaviour in the ferroelectric orthorhombic phase of $KNbO_3$ [33], where the longstanding discrepancy between Raman and INS studies was resolved only after a *coupled* damped harmonic oscillator analysis of the Raman and INS results [33].

3.3 Soft mode dispersion in the a*-b* plane

The low frequency phonon dispersion branches of $Sn_2P_2S_6$ in the a^*-b^* plane were studied on 1T1 (LLB, Saclay) at two temperatures (302 K in the ferroelectric phase, and 440 K in the paraelectric phase) with a typical energy resolution of 200 GHz, probing the soft branch dispersion along b^* as well as the behaviour of y-polarized phonons. In this way, the dispersion along the three main crystal

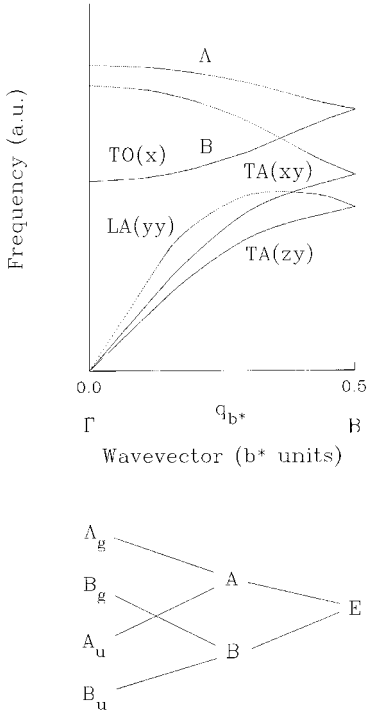

Fig. 7. Mode symmetry along the b^* direction in the paraelectric phase ($P2_1/n$). Solid lines represent B-type symmetry and dashed lines A-type symmetry modes.

directions has been obtained, as required for setting up a lattice dynamical model of the transition.

The symmetry of the lowest frequency phonon branches along the b^* direction are given in Figure 7 for the paraelectric phase. At the Γ point four different irreducible representations A_g, B_g, A_u and B_u exist. Along the b^* direction the modes are symmetric (A) or antisymmetric (B) with respect to the two-fold screw-axis. At $\frac{1}{2}b^*$, the modes are doubly degenerate (E). There are no symmetries left in the ferroelectric phase for modes propagating along b^*, except at the zone center (A' and A'' representations).

The experimental dispersion branches are given in Figure 8 (302 K) and Figure 9 (440 K). A clear TA(xy) phonon along b^* is observed in the (4 ζ 0) geometry, with a limiting slope (at 302 K) in agreement with ultrasound measurements of the sound velocity (295 K) [34]. When comparing its dispersion in the paraelectric phase to that in the ferroelectric phase, a strong frequency reduction at high ζ values is apparent, and simultaneously, its linewidth is significantly broader at 440 K. This indicates a repulsion because of coupling to the TO(x) soft optic branch.

The soft optic TO(x) phonon could be observed in the (5 1+ζ 0) zone, as shown in the spectra given in Figure 10. A clear frequency change of the soft mode (1.10 THz at 302 K *versus* 0.78 THz at 440 K for (5 1.15 0)) is seen, which is consistent with its temperature dependence at the Brillouin zone center (as discussed in Sect. 3.2).

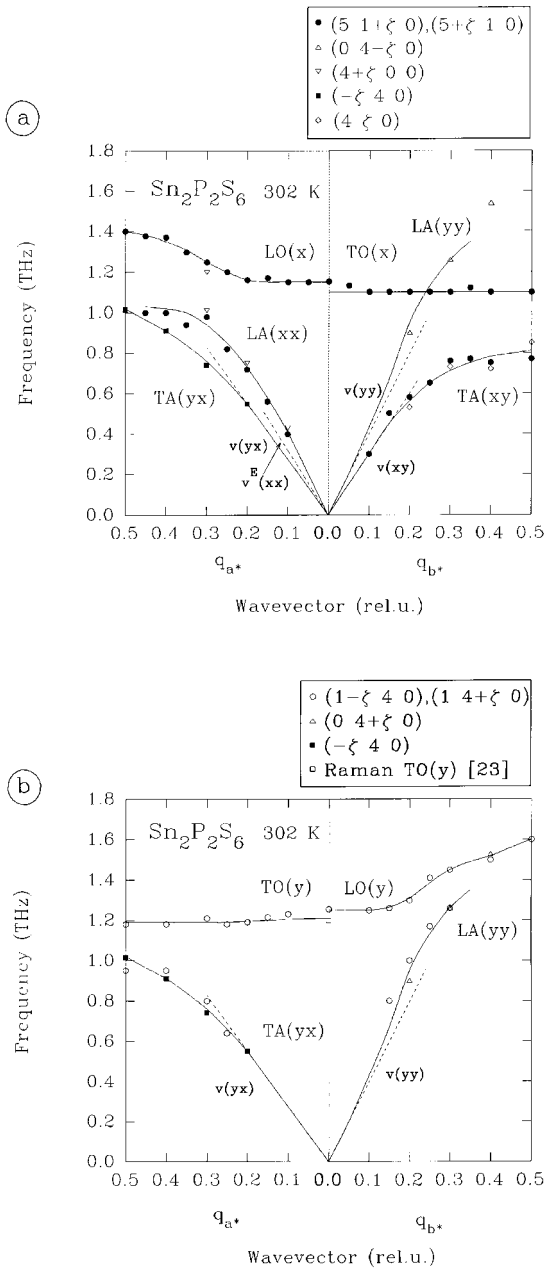

Fig. 8. Low frequency phonon dispersion branches in the ferroelectric phase of $Sn_2P_2S_6$ (302 K) (errorbars typically ±0.04 THz); (a) x-polarized soft optic mode and acoustic branches. (b) same for the y-polarization. Solid lines are guides to the eye.

The spectra showed that for higher values of ζ the modes present (TA(xy), TO(x) and another optic mode O1) start to overlap. At 302 K, the soft optic mode parameters were reliably extractable, with the TA(xy) frequencies close to the corresponding ones obtained in the (4 ζ 0) geometry. The linewidths and intensity variations as a function of ζ confirm that the TO(x) and TA(xy) phonons are coupled. Moreover, Figures 8 and 9 show that

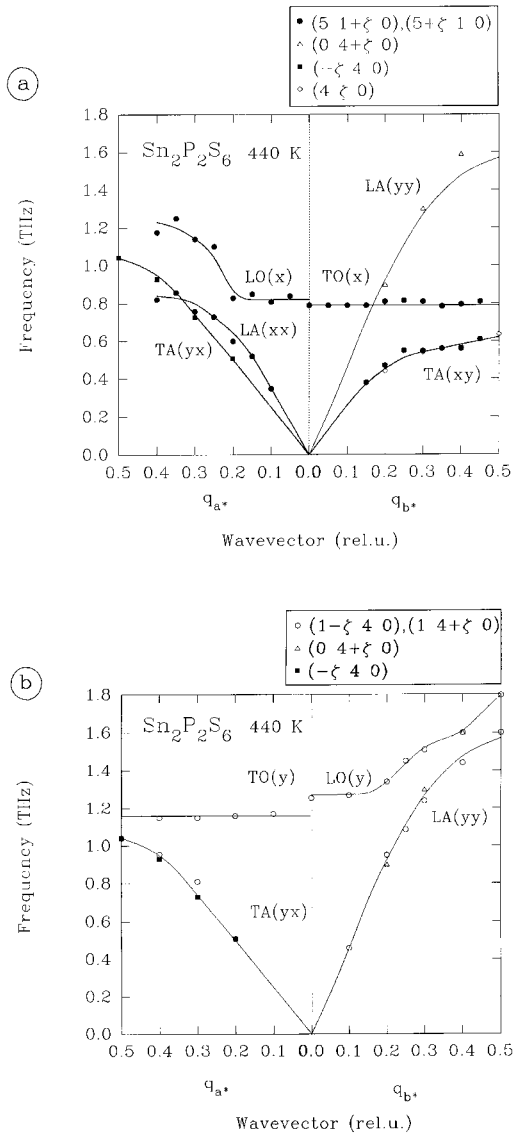

Fig. 9. Low frequency phonon dispersion branches in the paraelectric phase of $Sn_2P_2S_6$ (440 K) (errorbars typically ± 0.04 THz); (a) x-polarized soft optic and acoustic branches. Notice the pronounced lowering of the TO and LO frequencies with respect to Figure 8a. Both LA(xx) and TA(xy) are clearly repelled by the soft branches. (b) y-polarized optic and acoustic dispersions. Solid lines are guides to the eye.

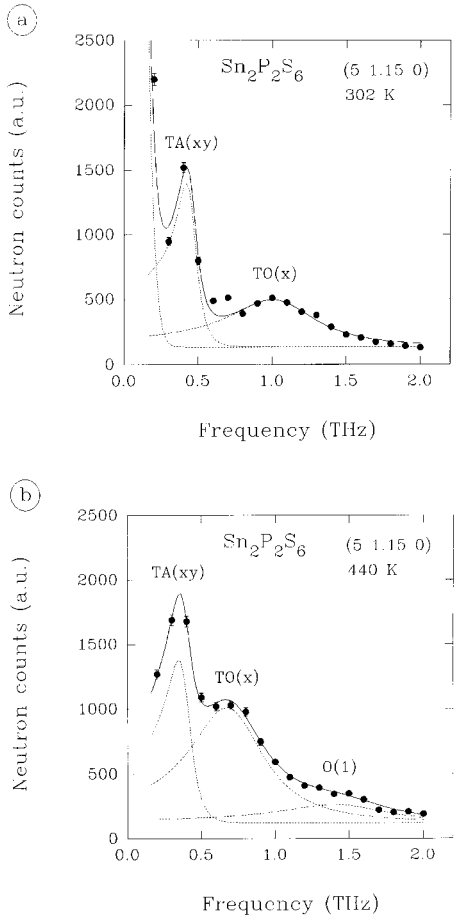

Fig. 10. Constant-Q spectra at $(5\ 1+\zeta\ 0)$ for $\zeta = 0.15$ (a) 302 K and (b) 440 K. A second optic mode (O1) is observed at 440 K in addition to the TA(xy) acoustic and TO(x) soft optic mode.

also the LO(x) and LA(xx) phonons are coupled, as evidenced by the branch repulsion. At the two experimental temperatures, the LO-TO splitting turns out to be rather low in both phases, with a value at 302 K consistent with the measurements in the a^*-c^* plane.

At 440 K, the broad response in the $(5\ 1+\zeta\ 0)$ geometry was analysed assuming the TA(xy) frequencies approximately at the values independently obtained in the $(4\ \zeta\ 0)$ geometry. Because of the broad response, the errorbars for the branch frequencies at high ζ values is larger (± 0.06 THz) at this temperature.

Interestingly, the soft branch dispersion seems to be qualitatively different along the b^* compared to the c^* direction, since along b^* the dispersion is rather flat, whereas the coupling between the acoustic and optic modes produces an upward bend of the dispersion curve along c^*. At 440 K, the soft branch remains quite flat along b^*, though it is clear from the spectra (intensity and linewidth transfer from the optic to the acoustic mode) and the temperature dependence of both branches, that the coupling between the acoustic and optic mode must be considerable. No indications of an instability along b^*, as suggested by previous lattice dynamical calculations [14], can be seen in the shape of the soft branch.

The y-polarized TO and LO optic phonons at about 1.2 THz could be followed in the $(1-\zeta\ 4\ 0)$ and $(1\ 4+\zeta\ 0)$ geometries, as shown in Figures 8 and 9. In the ferroelectric phase the branches are close to the soft branch, but, in contrast to the x-polarized optic mode, show almost no frequency change ($\delta\omega \leq 0.03$ THz) between the paraelectric and ferroelectric phase. The LO-TO splitting of this

mode is also quite small. The near temperature independence of the y-polarized mode is in agreement with Raman studies [23], with a frequency consistent with the present INS measurements (Fig. 8). The LO(y) mode shows, similar to the couplings observed for the soft mode, an interaction with the LA(yy) mode (A symmetry) along b^*.

3.4 Acoustic branches

The acoustic branches in the a^*-c^* plane shown in Figure 2 represent a TA (u_{xz}) phonon and two LA (u_{xx} and u_{zz}) phonons. The limiting slopes obtained from ultrasound velocities [18] $v(zz)$ (3.75×10^3 ms^{-1} at 295 K and 3.59×10^3 ms^{-1} at 330 K) and $v(xz)$ [34] (2.30×10^3 ms^{-1} (at 295 K)) agree well with the extrapolations of the neutron data towards $q = 0$ at all temperatures.

However, the slope corresponding to $v(xx)$ obtained from neutron scattering (about 4.26×10^3 ms^{-1} at 250 K) is substantially higher than the slope expected from the ultrasound velocity $v(xx)$ measurements (2.9×10^3 ms^{-1} at 70 MHz). A similar deviation was found in $Sn_2P_2Se_6$ (100 K) [5].

Two phenomena turn out to contribute to the difference. First, a strong dispersion in the ultrasound velocity $v(xx)$ occurs in the MHz-region, which has been related to domain relaxation. This relaxation does not extend to the THz-region. A good estimate for the final velocity without dispersion can be obtained from the ultrasound determination in the paraelectric phase, where domains are absent: $v(xx) = 3.05 \times 10^3$ ms^{-1} at 70 MHz.

Secondly, $Sn_2P_2S_6$ exhibits strong piezoelectric properties in the ferroelectric phase, which account for the remaining difference. The sound velocity is changed by the piezoelectric effect, if the induced electric dipole field $\mathbf{P}_{ind}$ of the acoustic displacement wave has a component along the propagation direction $\mathbf{q} = \mathbf{l}$ [35,36], leading to an increase in the effective restoring forces. Therefore, velocities are classified as v^E ($\mathbf{P}_{ind,l} = 0$, constant electric field $\mathbf{E}$ condition) and the (slightly) higher v^{D_l} ($\mathbf{P}_{ind,l} \neq 0$, constant electric displacement $\mathbf{D_l}$ condition).

The piezoelectric relation $\mathbf{P} = \mathbf{d}\boldsymbol{X}$ enables one to deduce the ultrasound velocity v^{D_l} from the piezoelectric modulus tensor $\mathbf{d}$ and the propagation direction $\mathbf{l}$ and strain field $\boldsymbol{X}$ of the acoustic phonon [37].

Here, the modifications to the ultrasound velocities (Tab. 1), to be used in the comparison with the neutron acoustic branches along a^* and c^* (Fig. 2), are calculated on the basis of the electromechanical coupling constants k_{lj} according to

$$v_{ij}^{D_l} = \frac{v_{ij}^E}{\sqrt{1 - k_{lj}^2}} \tag{4}$$

in which the electromechanical coupling constants are related to the piezoelectric moduli following:

$$k_{lj} = \frac{d_{lj}}{\sqrt{\frac{\epsilon_{ll}\epsilon_0}{C_{jj}}}} \tag{5}$$

Table 1. Piezoelectric corrections to the sound velocities v at 295 K.

q	k_{ij}	$v^E(10^3$ ms$^{-1})$	$v^D(10^3$ ms$^{-1})$
// a^*	$k_{11} = 0.67$	$v_{11}^E = 3.05$	$v_{11}^{D_1} = 4.11$
// c^*	$k_{33} = 0.15^+$	$v_{33}^E = 3.75$	$v_{33}^{D_3} = 3.79$
// c^*	$k_{35} = 0.39^+$	$v_{13}^E = 2.30$	$v_{13}^{D_3} = 2.50$
// a^*	$k_{15} = 0.10^+$	$v_{13}^E = 2.30$	$v_{13}^{D_1} = 2.31$

with $\epsilon_{ll}\epsilon_0$ and C_{jj} the corresponding dielectric constant and elastic compliance.

The electro-mechanical coupling constant k_{11} is relatively high: $k_{11} = 0.67$ at 295 K [38], which is reflected in the strong change in the sound velocity $v_{11}^{D_1}$. Using formula (4) a value of $v^D(xx) = 4.11 \times 10^3$ ms^{-1} at 295 K is obtained, in good agreement with the limiting slope of the neutron scattering data, thereby solving the remaining discrepancy.

The values for k_{11}, k_{12}, k_{13}, k_{31} and k_{32} and part of the piezoelectric modulus tensor $\mathbf{d}$ have been determined by Vysochanskii *et al.* [39]. The electromechanical coupling constants indicated in Table 1 by $^+$ have been estimated using formula (5). k_{33} was calculated from the known elastic compliances and coefficients k_{32}, d_{33} and d_{32} according to $k_{33} = \left(\frac{C_{33}}{C_{22}}\right)^{1/2} \left(\frac{d_{33}}{d_{32}}\right) k_{32}$. An estimation of the relative value of C_{55} and C_{22} allowed to calculate k_{15} and k_{35} in a similar manner.

The resulting ultrasound velocities $v_{ij}^{D_l}$ in Table 1 were used in Figure 2, where good consistency is obtained with respect to the limiting slopes on all four acoustic branches.

Along the b^* direction and for the y-polarized TA(yx) mode along a^*, the slopes obtained from ultrasound (295 K) and from the present neutron study at 302 K are consistent (Fig. 8). Here, indeed piezoelectric corrections are absent because the corresponding piezoelectric moduli, with b perpendicular to the glide plane of the Pn space group, vanish by symmetry.

4 Conclusions

The relationship between lattice dynamics and the ferroelectric phase transition has been studied for the proper ferroelectric $Sn_2P_2S_6$. The lattice dynamics in the a^*-c^* plane is studied in the ferroelectric phase, where a clear x-polarized soft optic mode is observed. In the paraelectric phase its softening is relatively slow, indicative of a mixed order-disorder/displacive transition, and stabilizes at about 0.6 THz around T_0. A question which could not be answered in the framework of this work is, whether or not this is accompanied by a central component, as in $Sn_2P_2Se_6$ [5] for the paraelectric-to-incommensurate transition.

The low frequency dispersion in both phases were obtained in the a^*-b^* plane, with consistent zone center soft mode frequency changes. Additional lattice dynamical calculations using the present information are expected

to provide a more microscopic insight in the nature of the forces leading to the phase transitions, in particular why an incommensurate phase appears in $Sn_2P_2Se_6$, and not in $Sn_2P_2S_6$.

An apparent inverted soft mode LO-TO splitting is observed at low temperatures, which can be related to coupling of the soft mode to the nearby P_z optical phonon. The related temperature dependence of the soft mode also indicates a pronounced coupling to the z-polarized optic mode, which seems to be at the origin of the anomalous anisotropy of the phonons observed in Raman spectroscopy.

An interaction between the soft TO(P_x) and TA(xz) acoustic modes is present in the ferroelectric phase, as evident from the dispersion and phonon lineshapes, quite similar to the interaction in the paraelectric phase of $Sn_2P_2Se_6$ [5]. Clearly, the x- and y-polarized optic phonons show distinct interactions with the acoustic phonons.

Consistency between the sound velocities obtained from ultrasonic measurements and from the limiting slopes in the neutron scattering study is obtained when including piezoelectric corrections.

One of us, S.W.H. Eijt, likes to thank the Dutch Organisation for Fundamental Research on Matter (FOM) for financial support. The Institut Laue-Langevin and the Laboratoire Léon Brillouin (Human Capital Mobility Program) are gratefully acknowledged for financial support during the visits of Yu.M. Vysochanskii and S.W.H. Eijt . The authors acknowledge the technical support by P. Boutrouille and A. Brochier.

References

1. J. Harada, J.D. Axe, G. Shirane, Phys. Rev. B **4**, 155 (1971).
2. A.H. Moudden, F. Denoyer, J.P. Benoit, W. Fitzgerald, Solid State Comm. **28**, 575 (1978).
3. W. Brill, K.-H. Ehses, Jpn J. Appl. Phys. **S-24**, 826 (1985).
4. Y. Yamada, I. Shibuya, S. Hoshino, J. Phys. Soc. Jpn **18**, 1594 (1963); A. Yamamoto, Phys. Rev. B **31**, 5941 (1985).
5. S.W.H. Eijt, R. Currat, J.E. Lorenzo, P. Saint-Grégoire, T. Janssen, B. Hennion, Yu.M. Vysochanskii, J. Phys-Cond. **10**, 4811 (1998).
6. A.P. Levanyuk, D.G. Sannikov, Sov. Phys. Solid State **18**, 1122 (1976).
7. Z.Y. Chen, M.B. Walker, Phys. Rev. Lett. **65**, 1223 (1990).
8. A.V. Gommonai, A.A. Grabar, Yu.M. Vysochanskii, A.D. Belyaev, V.F. Machulin, M.I. Gurzan, V.Yu. Slivka, Sov. Phys.-Solid State **23**, 2093 (1981).
9. B. Dorner, *Coherent Inelastic Neutron Scattering and Lattice Dynamics*, Spinger Series in Solid State Sciences, Vol. 34, (Springer Verlag, Berlin, 1980) p 68.
10. G. Dittmar, H. Schaeffer, Z. Naturforsch. **29b**, 312 (1974).
11. F. Scott, M. Pressprich, R.D. Willert, D.A. Cleary, J. Solid State Chemistry **96**, 294 (1992).
12. R. Israel, S.W.H. Eijt, R. de Gelder, J.M.M. Smits, P.T. Beurskens, Th. Rasing, H. van Kempen, M.M. Maior, S.F. Motrija, Z. Kristallogr. **213**, 34 (1998).
13. Yu.V. Voroshilov, M.N. Portorii, L.A. Seikovskaya, A.V. Yatsenko, I.P. Prits, Sov. Phys. Crystallogr. **33**, 761 (1988).
14. V.M. Rizak, Yu.M. Vysochanskii, A.A. Grabar, V. Yu. Slivka, Sov. Phys. Solid State **31**, 1185 (1990).
15. Yu.M. Vysochanskii, V.Yu. Slivka, A.P. Buturlakin, M.I. Gurzan, D.V. Chepur, Sov. Phys. Solid State **20**, 49 (1978).
16. A.A. Volkov, G.V. Kozlov, N.I. Afanas'eva, Yu.M. Vysochanskii, A.A. Grabar, V.Yu. Slivka, Sov. Phys. Solid State **25**, 1482 (1983).
17. J. Grigas, V. Kalesinskas, S. Lapinskas, M.I. Gurzan, Phase Transitions **12**, 263 (1988).
18. V.D. Valevichius, Sov. Phys. Solid State **29**, 3703 (1987).
19. V.D. Valevichius, V.I. Samulenis, Yu.M. Vysochanskii, M.M. Maior, M.I. Gurzan, Sov. Phys. Solid State **31**, 1180 (1989).
20. A.I. Ritus, N.S. Rislik, Yu.M. Vysochanskii, A.A. Grabar, V.Yu. Slivka, Sov. Phys. Solid State **27**, 1337 (1985).
21. M.M. Maior, B.M. Koperles, B.A. Savchenko, M.I. Gurzan, O.V. Morozova, N.F. Korda, Sov. Phys. Solid State **25**, 117 (1983).
22. A.V. Gommonai, Yu.M. Vysochanskii, V.Yu. Slivka, Sov. Phys. Solid State **24**, 606 (1982).
23. A.V. Gommonai, Yu.M. Vysochanskii, A.A. Grabar, V.Yu. Slivka, Sov. Phys. Solid State **23**, 2105 (1982).
24. V.Yu. Slivka, Yu.M. Vysochanskii, M.I. Gurzan, D.V. Chepur, Sov. Phys. Solid State **20**, 2042 (1978).
25. V.Yu. Slivka, Yu.M. Vysochanskii, M.I. Gurzan, D.V. Chepur, Sov. Phys. Solid State **21**, 1378 (1979).
26. J.C. Decius, R.M. Hexter, *Molecular Vibrations in Crystals*, (McGraw-Hill, New-York, 1977).
27. H. Bilz, W. Kress, *Phonon Dispersion Relations in Solids*, Springer Series in Solid State Sciences, Vol. 10, (Springer Verlag, Berlin, 1979).
28. M. Born, K. Huang, *Dynamical Theory of Crystal Lattices*, (Oxford University Press, Oxford, UK, 1954).
29. Yu.M. Vysochanskii, V.Yu. Slivka, Sov. Phys.-Usp. **35**, 123 (1992).
30. S. Padlewski, A.K. Evans, C. Ayling, V. Heine, J. Phys-Cond. **4**, 4895 (1992).
31. K. Tani, J. Phys. Soc. Jpn **26**, 93 (1969).
32. A.A. Grabar, Yu.M. Vysochanskii, V.G. Furtsev, V.M. Rizak, V.Yu. Slivka, Ukr. Fiz. Zhur. **31**, 908 (1986).
33. R. Currat, H. Buhay, C.H. Perry, A.M. Quittet, Phys. Rev. B **40**, 10741 (1989).
34. Yu.M. Vysochanskii *et al.*, Department of Physics and Chemistry of Solid State, Uzhgorod State University (unpublished).
35. I. Koga, M. Aruga, Y. Yoshinaka, Phys. Rev. **109**, 1467 (1958).
36. R. Currat, R. Comès, B. Dorner, E. Wiesendanger, J. Phys. C: Solid State Phys. **7**, 2521 (1974).
37. W. Cady, *Piezoelectricity*, (Van Nostrand, New York, 1946).
38. M.M. Maior, P.H.M. van Loosdrecht, H. van Kempen, Th. Rasing, S.B. Molnar, S.F. Motrij, J. Phys-Cond. **5**, 6023 (1993).
39. Yu.M. Vysochanskii, M.I. Gurzan, M.M. Maior, E.D. Rogach, F.I. Savenko, V.Yu. Slivka, Sov. Phys. Crystallogr. **35**, 459 (1990).